Research on the vortical and turbulent structures in the lobed jet flow using laser induced fluorescence and particle image velocimetry techniques

To cite this article: Hui Hu *et al* 2000 *Meas. Sci. Technol.* **11** 698

View the article online for updates and enhancements.

Research on the vortical and turbulent structures in the lobed jet flow using laser induced fluorescence and particle image velocimetry techniques

Hui Hu, Tetsuo Saga, Toshio Kobayashi and Nubuyuki Taniguchi

Institute of Industrial Science, University of Tokyo, 7-22-1 Roppongi, Tokyo 106-8558, Japan

E-mail: `huhui@cc.iis.u-tokyo.ac.jp`, `saga@iis.u-tokyo.ac.jp`,
`kobaya@iis.u-tokyo.ac.jp` and `ntani@iis.u-tokyo.ac.jp`

Abstract. The changes in vortical and turbulent structure in the near field ($X/D < 3.0$) of jet mixing flow caused by a lobed nozzle were investigated experimentally in the present study. The techniques of planar laser induced fluorescence and particle image velocimetry were used to accomplish flow visualization and velocity field measurements. The experimental results showed that, compared with a circular jet flow, lobed jet mixing flow was found to have a shorter laminar region, a smaller scale of the spanwise Kelvin–Helmholtz vortices, earlier appearance of small scale turbulent structures and a larger region of intensive mixing in the near field of the jet mixing flow. The central line velocity decay of the lobed jet mixing flow was also found to be much faster than that in a conventional circular jet. All these indicated that the lobed nozzle provides better mixing performance than does a conventional circular nozzle.

Keywords: jet mixing flow, mixing enhancement, lobed nozzle, particle image velocimetry, laser induced fluorescence

(Some figures in this article are in colour only in the electronic version; see `www.iop.org`)

1. Introduction

The physics of mixing layers is of considerable interest both from fundamental and from practical points of view. It has been suggested that mixing is intimately connected with the transient of turbulence. In engineering flows, the process of mixing governs the rate of mixing in combustion chambers, the jet noise level of airplanes and vehicles and the spread of pollutants at industrial sites. Research into the physics of mixing and the mechanisms for enhancing mixing is necessary for many engineering applications, for example for improving combustion efficiency, suppressing jet noise and reducing the size of such functional devices.

During the past decades, it has become clear that an enormously powerful mechanism for enhancing flow mixing is the generation of streamwise vortices in a mixing flow by using some vortex generators such as lobed nozzles. Investigating the evolution of various vortices in a lobed jet mixing flow and the interaction among these vortices in order to reveal the differences of turbulent and vortical structures in a lobed jet mixing flow from those in a conventional circular jet is the subject of the present study.

A lobed nozzle, which consists of a splitter plate with a convoluted trailing edge, is an extraordinary fluid mechanics

device for efficient mixing of two co-flowing streams with different velocities, temperatures and/or spieces. Such a device had been known since the earliest days of jet engines and has received considerable attention with the aim of reducing jet noise since the 1960s. More recently, use of a lobed nozzle has emerged as an attractive approach for mixing the core and bypass streams of turbofan engines in order to improve propulsion efficiency, reduce the specific fuel consumption (SFC) and suppress the emission of infrared radiation (Power *et al* 1994, Presz *et al* 1994, Hu *et al* 1996). Lobed nozzles/mixers have also received attention for use in supersonic ejectors to reduce jet noise at take off and landing of aircraft as well as in combustion chambers for enhancing mixing between fuel and air (Tillman and Presz 1993, Smith *et al* 1997).

Among the researchers who worked to reveal the mechanism of the enhancement of mixing with a lobed nozzle/mixer, Paterson (1982) was the first to measure the velocity and turbulent characteristics downstream of a lobed nozzle/mixer systemically by using laser Doppler velocimetry (LDV). He concluded that a lobed nozzle/mixer could cause large-scale streamwise vortices to be shed at the trailing edges of lobes. So the downstream part of the flow field has many arrays of large-scale streamwise
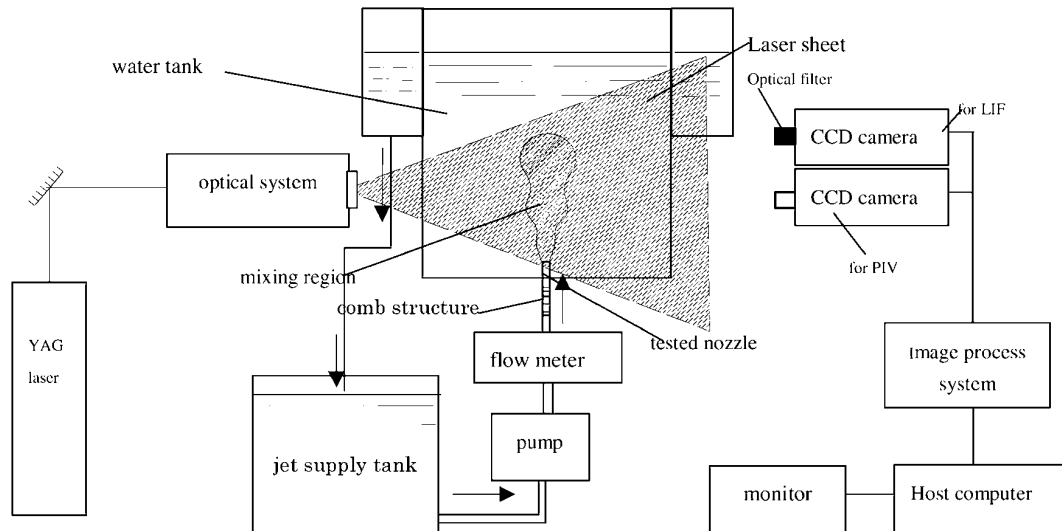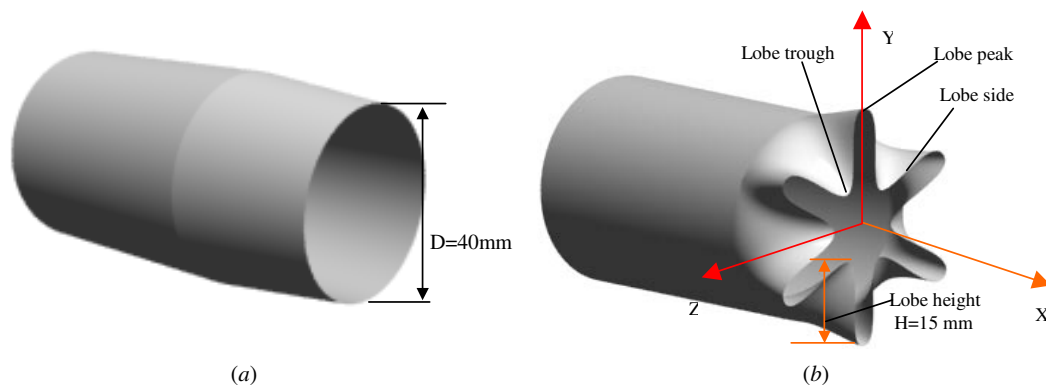
Figure 1. The experimental set-up.

Figure 2. The test nozzles ((a) circular and (b) lobed) and three axial slices studied.

vortices of alternating sign, which are believed to be primarily responsible for the enhancement of mixing.

Much of the later work on lobed nozzles concentrated on discovering the underlying physics of the lobed mixing. The work of Werle *et al* (1987) and Eckerle *et al* (1990) suggested that the process of formation of the large-scale streamwise vortices is an inviscid one, which was proposed to take place in three basic steps: vortices form, intensify and rapidly break down into small-scale turbulent structures.

Elliott *et al* (1992) found that both the streamwise vortices shed from a lobed trailing edge and the increase in initial interfacial area associated with the use of lobe geometry are significant for increasing the mixing compared with that occurring within a conventional flat plate splitter. At velocity ratios close to 1.0, the increase in mixing is due mainly to the increase in contact area, whereas the streamwise vortices have a larger role at a velocity ratio of 2.0 and its importance rises as the velocity ratio increases.

The study by McCormick and Bennett (1994) revealed more details about the flow patterns downstream of a lobed nozzle/mixer. On the basis of pulsed-laser sheet flow visualization with smoke and three-dimensional velocity measurements with a hot film anemometer (HFA), they suggested that the interaction of Kelvin–Helmholtz

(spanwise) vortices with the streamwise vortices produces the high levels of mixing. The streamwise vortices deform the normal vortices into pinch-off structures and increase the effect of stirring in the mixing flow. These effects result in the creation of intense small-scale turbulence and mixing.

Ukeiley *et al* (1992, 1993) and Glauser *et al* (1996) measured a planar lobed mixer flow field by using a rake of hot wires. On the basis of proper orthogonal decomposition (POD) analysis and pseudo-flow visualization (PFV) of the data from the hot wire rake, they suggested that the turbulence dominated mixing in the lobed mixer flow field is due to the collapse of the pinch-off shear layer. The collapse of the shear layer onto itself, which occurred at a distance downstream of 3–6 times the lobe height, induced a burst of energy characterized by a region or pocket of high turbulence intensity.

Belovich and Samimy (1997), summarized the results of previous research by stating that the mixing in a lobed nozzle/mixer is controlled by three primary elements. The first is the streamwise vortices generated due to the lobed shape, the second is the increase in interfacial area between the two flows due to the special geometry of lobed structures and the third is the Brown–Roshko type structures which
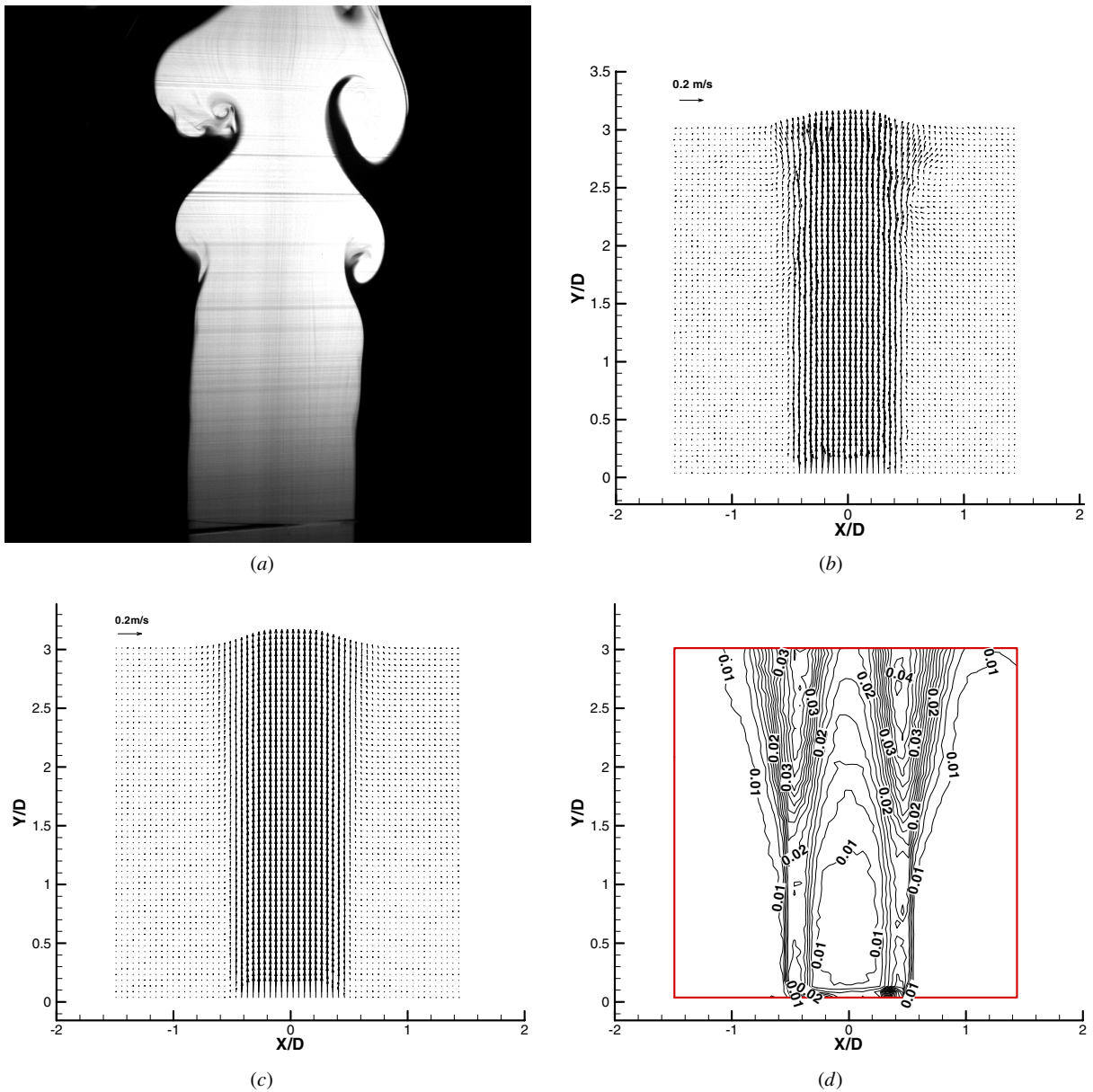
(*a*)

(*b*)

(*c*)

(*d*)

Figure 3. LIF visulization and PIV measurement results for the circular jet mixing flow ($Re = 6000$): (*a*) LIF visualization, (*b*) instantaneous PIV result, (*c*) the mean velocity distribution obtained by PIV and (*d*) the turbulence intensity distribution.

occur in any shear layer due to the Kelvin–Helmholtz instabilities.

Although many important results have been obtained through these investigations, much work was still needed in order to more clearly understand the fluid dynamic mechanism of the enhancement of mixing by a lobed nozzle/mixer. This was especially true regarding the differences of vortical and turbulent structure in a lobed jet mixing flow compared to those in a conventional jet flow. Most of the previous research was conducted by using a Pitot probe, LDV or a HFA, with which it is very hard to reveal the vortical and turbulent structures in lobed jet mixing flows instantaneously and globally due to the limitations of these experimental techniques. In the present study, both planar laser induced fluorescence (LIF) and particle image velocimetry (PIV) techniques were used to study

the lobed jet mixing flows instantaneously and globally. The evolution of spanwise Kelvin–Helmholtz vortices and their interactions with streamwise vortices in the lobed jet mixing flow were studied by using the directly perceived LIF flow visualization images and velocity field and the derived, vorticity distributions and turbulence intensity distributions of PIV measurement results. The changes of the turbulent and vortical structures in the near field of jet mixing flow caused by a lobed nozzle are discussed in detail.

2. The experimental set-up

Figure 1 shows schematically the experimental set-up used in the present study. The test nozzles were installed in the middle of the water tank (600 mm × 600 mm × 1000 mm). Fluorescent dye (rhodamine B) for LIF or PIV tracers
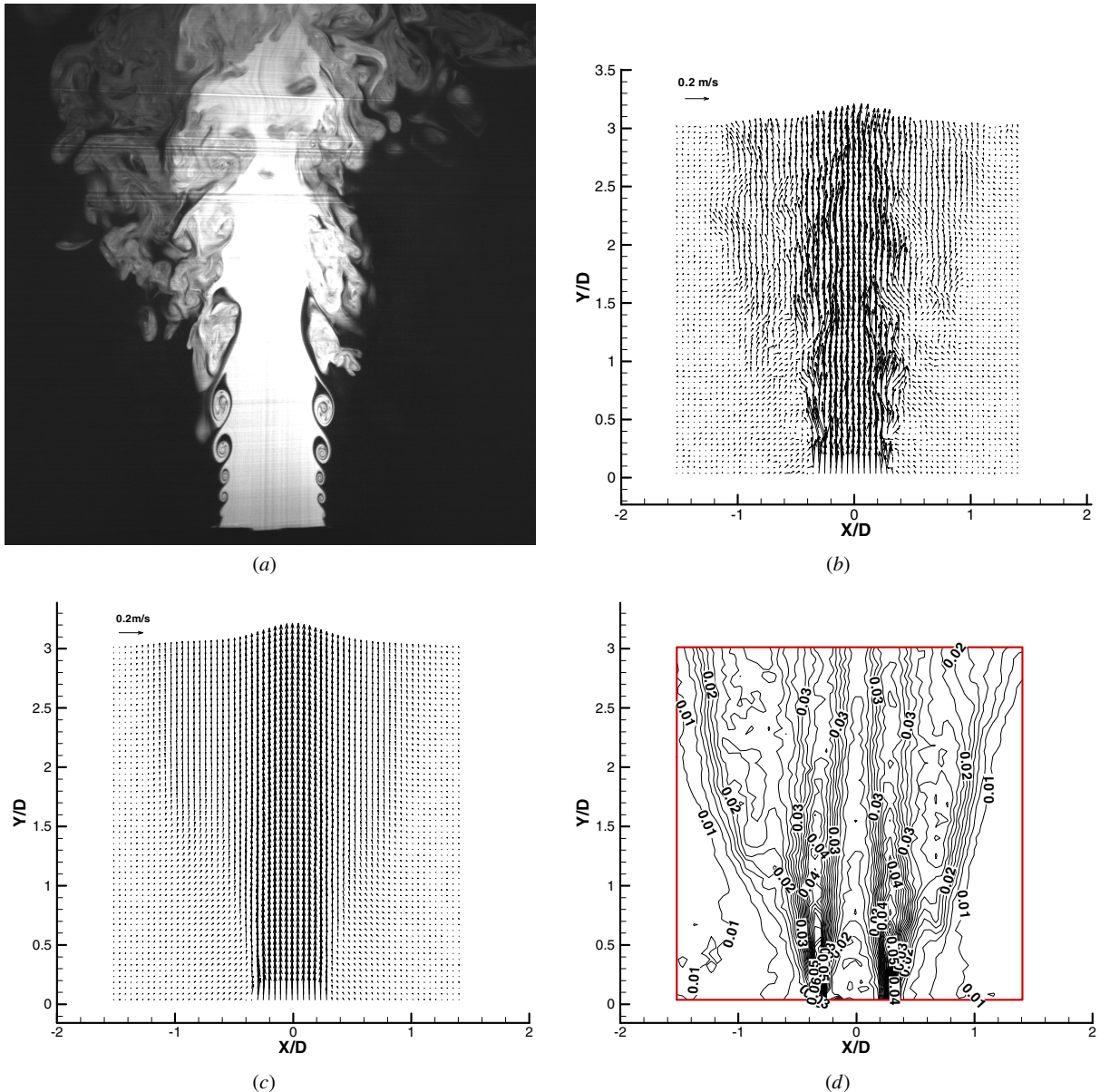
Figure 4. LIF visualization and PIV measurement results for lobed jet mixing flow in the lobe trough slice ($Re = 6000$): (*a*) LIF visualization, (*b*) instantaneous PIV result, (*c*) the mean velocity distribution obtained by PIV and (*d*) the turbulence intensity distribution.

(polystyrene particles of diameter $d = 20–30\,\mu$m and density $1.02\,\text{kg cm}^{-3}$) was premixed with water in the jet supply tank and jet flow was supplied by a pump. The flow rate of the jet, which was used to calculate the representative velocity and Reynolds numbers, was measured by a flow meter. A contraction and honeycomb structures were installed at the inlets of test nozzles to ensure that the turbulence intensity levels of jet flows at the exits of test nozzles were less than 3%.

The pulsed-laser sheet (of thickness about 1.0 mm) used for LIF visualization and PIV measurement was supplied by twin Nd:YAG lasers with the frequency of 10 Hz and power of 200 mJ per pulse. The time interval between the two pulses was adjustable. A 1008 by 1016 pixels cross-correlation CCD array camera (PIVCAM 10-30) was used to capture the LIF and PIV images. The twin Nd:YAG lasers and the CCD camera were controlled by a synchronizer control system. The LIF and PIV images captured by the CCD camera were

digitized by an image processing board and then transferred to a work station (CPU 450 MHz, RAM 1024 MB, HD20GB) for image processing and displayed on a PC monitor.

Rhodamine B was used as the fluorescent dye in the present experiment. The fluorescent light ($\lambda_f = 590$ nm) was separated from the scattered laser light ($\lambda_l = 532$ nm) by installation of a high pass optical filter at the head of the CCD camera. A low concentration rhodamine B solution (0.5 mg l^{-1}) was used to ensure that the strength of the fluorescent light was linear with respect to the concentration of the fluorescent dye and that the effect of laser light attenuation as the laser light sheet propagated through the flow was negligible (Hu *et al* 1999).

For the PIV image processing, rather than tracking individual particles, the cross-correlation method (Willert and Gharib 1991) was used in the present study to obtain the average displacement of the ensemble of particles. The
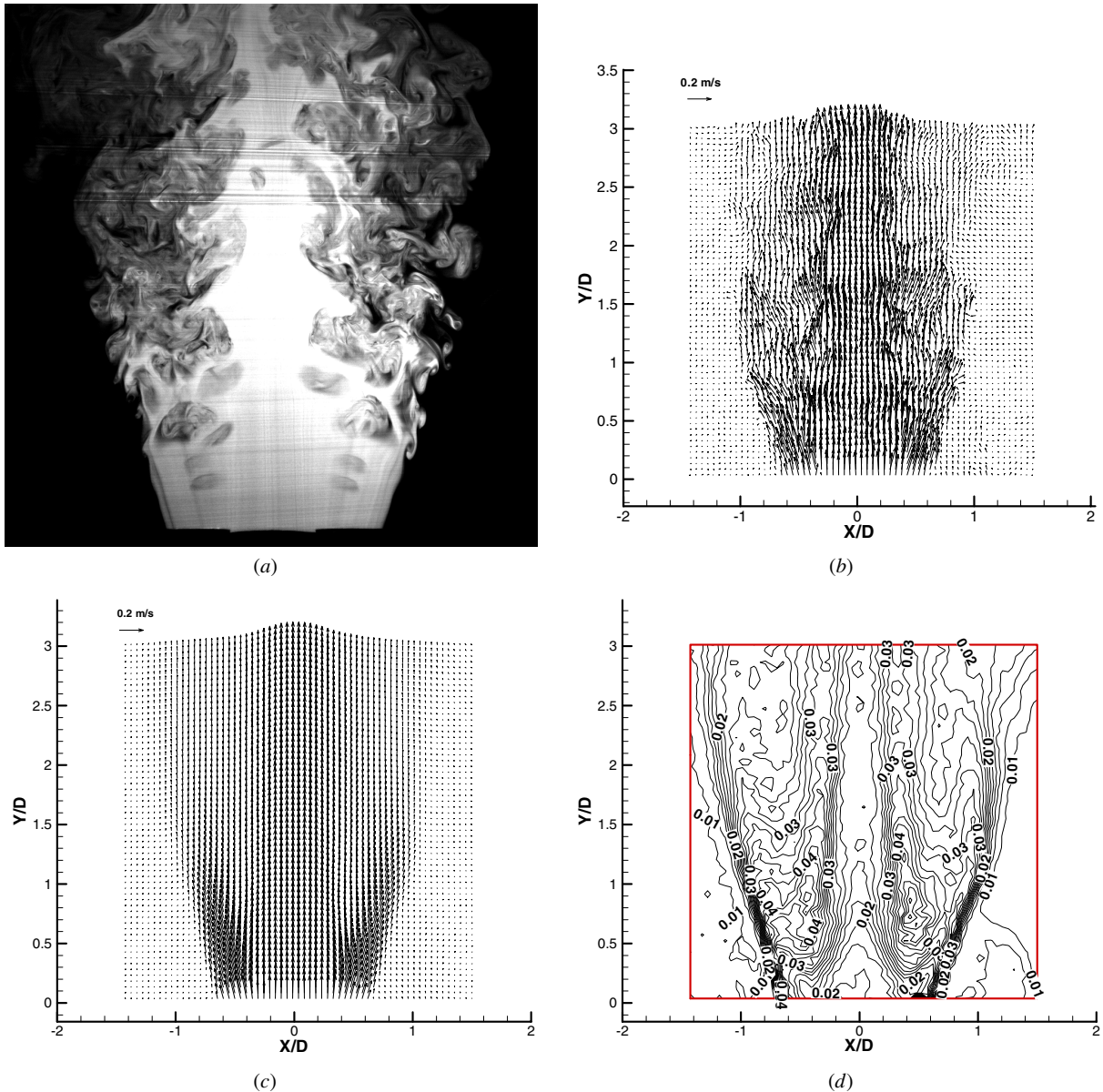
Figure 5. LIF visualization and PIV measurement results for lobed jet mixing flow in the lobe peak slice ($Re = 6000$): (*a*) LIF visualization, (*b*) instantaneous PIV result, (*c*) the mean velocity distribution obtained by PIV and (*d*) the turbulence intensity distribution.

images were divided into 32 by 32 pixel interrogation windows and 50% overlap grids were employed. The resolution the PIV images for the present research is about 120 μm per pixel. The post-processing procedures, which included sub-pixel interpolation (Hu *et al* 1998) and deletion of spurious velocities (Westerweel 1994), were used to improve the accuracy of the PIV result.

Figure 2 shows the two test nozzles used in the present study; namely a baseline circular nozzle and a lobed nozzle with six lobes. The height of the lobes is 15 mm ($H = 15$ mm). The inner and outer penetration angles of the lobe structures are about $22°$ and $14°$ respectively. The equivalent diameters of the two nozzles at the exit were designed to be the same, i.e. $D = 40$ mm. In the present study, the jet velocities (U_0) were set to be about 0.1 and 0.2 m s^{-1}. The Reynolds numbers of the jet flows were calculated from the nozzle exit diameter and the jet velocities

to be about 3000 and 6000.

In the present study, the differences in turbulent and vortical structures in a lobed jet mixing flow from those in a conventional circular jet flow in the axial slices were investigated first of all. The three axial slices studied for the lobed jet mixing flow are the lobe trough slice (the X–Z plane), lobe peak slice (the X–Y plane) and lobe side slice. Then, the LIF flow visualization and PIV measurement at several cross sections for the lobed jet mixing flow and conventional circular jet flow were also conducted in order to reveal the differences between the vortical and turbulent structures in the cross planes of the jet mixing flows of these two types.

For the PIV measurement results, the time average values, which include the mean velocity vectors, mean streamwise vorticity distributions and mean turbulence intensity ($T_{i,j} = [RMS(u_{i,j})^2 + RMS(v_{i,j})^2]^{1/2}$) fields in the laser sheet planes, were used to compare the mixing
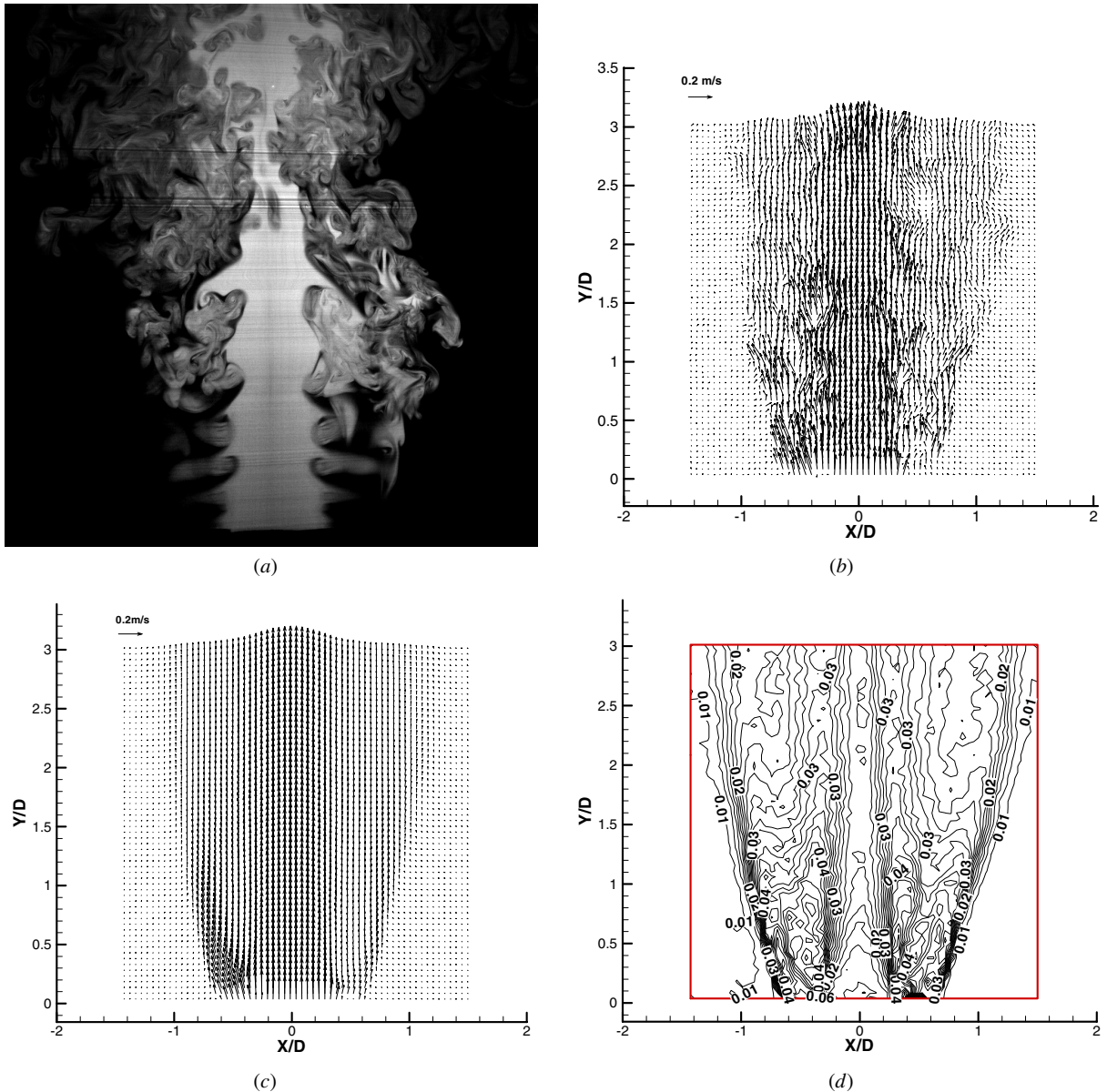
Figure 6. LIF visualization and PIV measurement results for lobed jet mixing flow in the lobe side slice ($Re = 6000$): (*a*) LIF visualization, (*b*) instantaneous PIV result, (*c*) the mean velocity distribution obtained by PIV and (*d*) the turbulence intensity distribution.

characteristics in the lobed jet mixing flows with those in conventional circular jet flow. These mean values were calculated using the average of 400 frames of the instantaneous PIV velocity fields, which were obtained at the frequency of 10 Hz.

It had been found that intensive mixing of the core jet flow with ambient flows could be achieved in the very near field of a jet flow by using a lobed nozzle/mixer. So, the CCD camera view of the present study was focused on the near region ($X/D < 3.0$) of the jet mixing flows.

3. Results and discussion

3.1. In the axial slices

Figure 3 shows the LIF flow visualization and PIV measurement results for the axial slice of a conventional circular jet at

the Reynolds number of 6000. From the LIF flow visualization result (figure 3(*a*)) and PIV instantaneous velocity field (figure 3(*b*)), it can be seen that there is a laminar region in the circular jet flow downstream of the circular nozzle. At the end of the laminar region ($X/D = 2.0$), spanwise Kelvin–Helmholtz vortices were found to roll up. Pairing and combining of these spanwise vortices and the transition of the jet flow to turbulence were found to occur much further downstream ($X/D = 4.0$–6.0), which is outside the CCD camera view of the present study. None of the small-scale turbulent and vortical structures can be found in the region investigated ($X/D < 3.0$) for the circular jet flow. The LIF visualization result obtained in the present study is very similar to the result reported by Liepmann and Gharib (1992).

From the PIV mean velocity field (figure 3(*c*)) and turbulence intensity distribution (figure 3(*d*)) at the same Reynolds number, it can be seen that the circular jet flow does
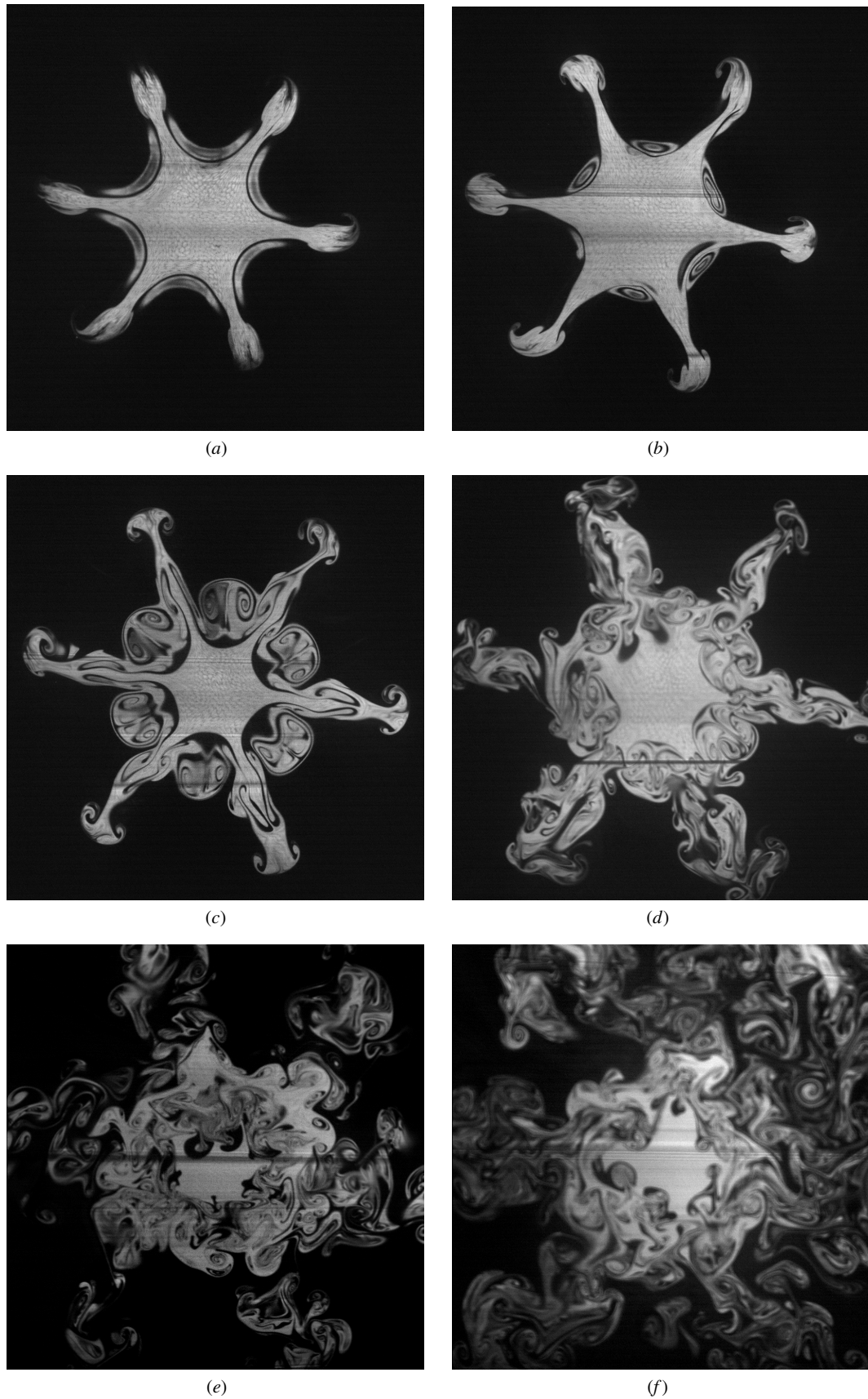
Figure 7. LIF visualization of the lobed jet mixing flow in several cross planes ($Re = 3000$): (*a*) $X = 10$ mm, (*b*) $X = 20$ mm, (*c*) $X = 30$ mm, (*d*) $X = 40$ mm, (*e*) $X = 60$ mm and (*f*) $X = 80$ mm.
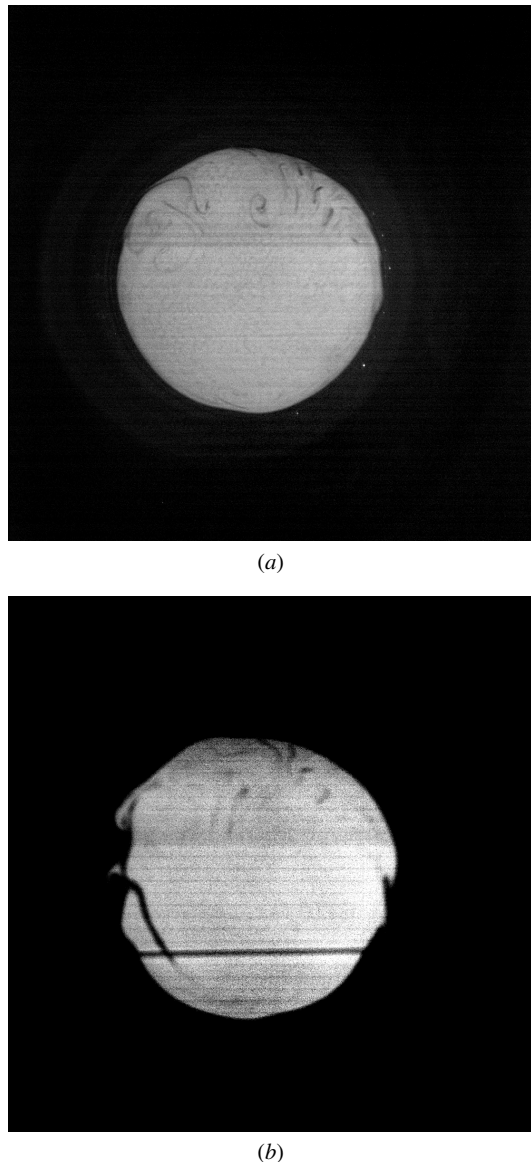
(a)

(b)

Figure 8. LIF visualization of the circular jet mixing flow in two cross planes ($Re = 3000$): (a) $X = 40$ mm and (b) $X = 80$ mm.

phenomena in a planar lobed mixing flow. Some small-scale turbulent and vortical structures, which indicate the intensive mixing of the core jet flow with ambient flow, were found to appear in the flow field downstream of $X/D = 1.0$.

From the PIV time average results (figures 4(b) and (c)) for this axial slice, it can also be seen that the lobed jet flow began to expand almost immediately after the exit of the lobed nozzle. The angle of expansion of the lobe jet mixing flow was found to be bigger than that in the conventional circular jet flow. The bigger high-turbulence-intensity regions (the regions of turbulence intensity exceeding 0.03 m s^{-1} in the figure 4(d)) can be found to concentrate in the near field of the lobed jet mixing flow. The potential core region (the regions of turbulence intensity less than 0.02 m s^{-1} in figure 4(d)) at the centre of the lobed jet flow was much smaller and shorter than that in the circular jet flow (figure 3(d)).

Figure 5 shows the LIF flow visualization and PIV measurement results in the lobed jet mixing flow for the axial slice passing the lobe peak (the X–Y plane, figure 2). The laminar region at the exit of the lobed nozzle in this axial slice was not a straight cylinder like that in the circular jet (figure 3(a)), but looked like an expansive cut-off cone downstream of the lobe structure instead. Compared with that in the lobe trough slice, the laminar region in the lobe peak axial slice was a bit longer ($X/D = 0.5$), but it was still much shorter than that in the circular jet mixing flow. This may be because the thickness of the boundary layer at the exit of the lobed nozzle was different (the work of Brink and Foss (1993) had verified that the thickness of the boundary layer at the lobe trough is smaller than that in the lobed peak) and the thicker boundary layer at the lobe peak needs a longer streamwise distance to roll-up the Kelvin–Helmholtz vortices (Hussain and Husain 1989). In this axial slice, it can also be seen that small-scale turbulent and vortical structures were found to appear in the flow field downstream of $X/D = 1.0$. From the PIV time average results (figures 5(c) and (d)), it can be seen that most of the high-turbulence-intensity regions were concentrated in the near field of the lobed jet mixing flow. The potential core region at the centre of the lobed jet mixing flow for this axial slice is also much smaller and shorter than that in the circular jet mixing flow shown in figure 3.

Figure 6 gives the LIF flow visualization and PIV measurement results for the lobed jet mixing flow in the axial slice passing the lobe side plane. In this slice, some streak flow structures can be seen clearly downstream of the trailing edge of the lobe structure. These structures were the Kelvin–Helmholtz vortical tubes shed periodically from the trailing edge of the lobe. This phenomenon was observed and in a planar lobe mixing flow called a 'normal vortex' by McCormick and Bennett (1994). Downstream of the location $X/D = 1.0$, small-scale turbulent and vortical structures were found to appear in the flow field. Just like in the lobe trough and lobe peak axial slices, most of the high intensity regions were found to concentrate in the near field of the lobed jet mixing flow. The potential core region at the centre of the lobed jet mixing flow in this axial slice was also much smaller and shorter than that in the circular jet.

not expand until the spanwise Kelvin–Helmholtz vortices began to roll up at about $X/D = 2.0$ downstream. A low turbulence intensity region (the region of turbulence intensity less than 0.02 m s^{-1} in figure 3(d)) can be found in the central region of the circular jet flow, which is called the potential core region for the jet flow. In the circular jet flow, it was found to extend to $X/D = 3.0$ downstream.

Figure 4 shows the LIF visualization and PIV measurement results of the lobed jet mixing flow in the axial slice passing the lobe trough (the X–Z plane, figure 2). Compared with the circular jet flow (figure 3), the laminar region of the lobed jet mixing flow was much shorter in this axial slice (figures 4(a) and (b)). The spanwise Kelvin–Helmholtz vortices were found to roll up almost immediately after the trailing edge of the lobed nozzle. It can also be found that these spanwise Kelvin–Helmholtz vortices were much smaller than those in the circular jet mixing flow (figure 3(a)). McCormick and Bennett (1994) had also observed the same
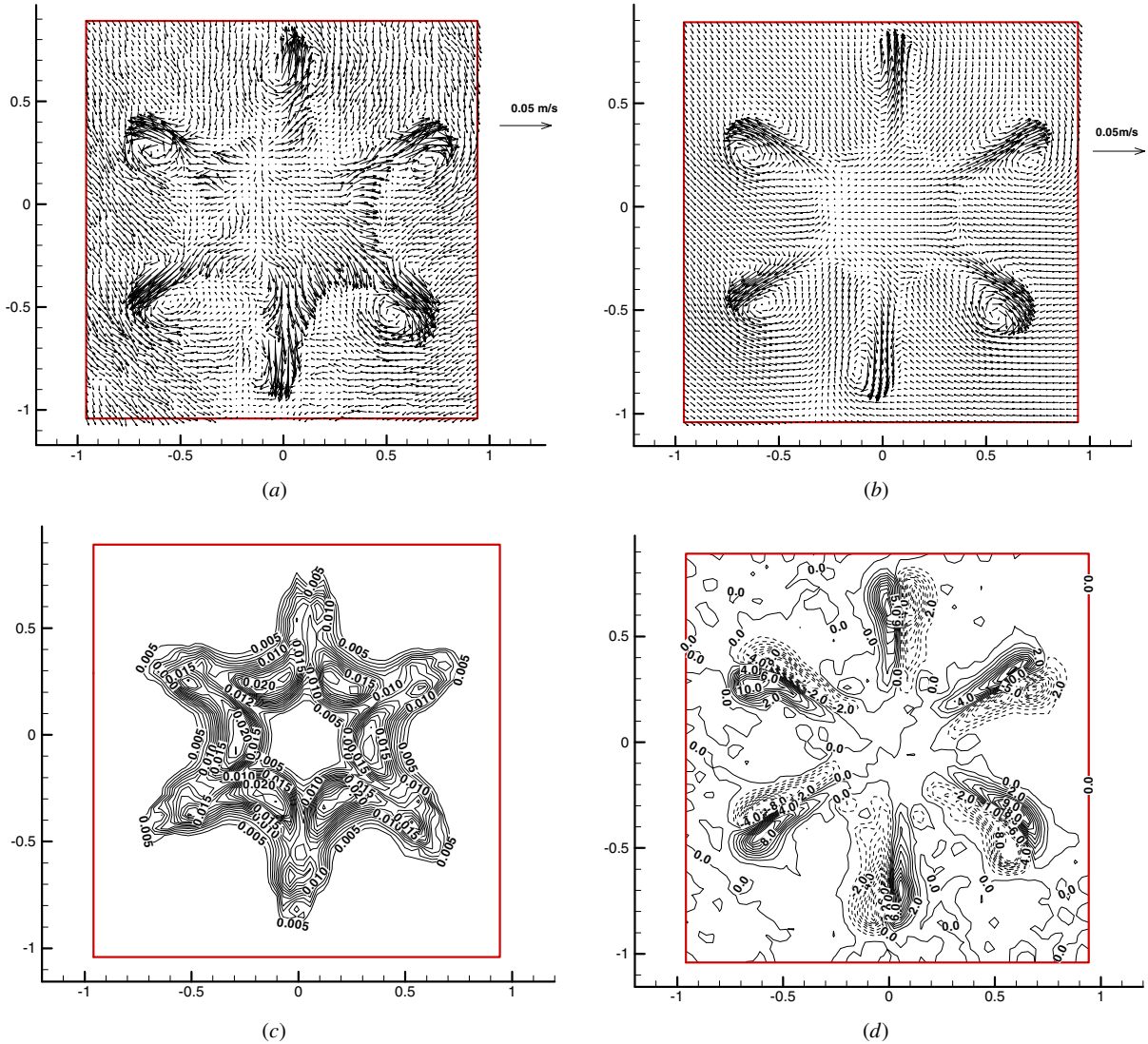
Figure 9. PIV measurement results for the lobed jet mixing flow ($Re = 3000$) for $X = 20$ mm: (*a*) the instantaneous velocity field, (*b*) the mean velocity field, (*c*) the turbulence intensity distribution and (*d*) the mean streamwise vorticity distribution.

3.2. In the cross planes

Figure 7 shows the LIF flow visualization results for the lobed jet mixing flow in six cross planes. At the downstream locations of $X/D = 0.25$ ($X/H = 0.7$, figure 7(*a*)) and $X/D = 0.50$ ($X/H = 1.3$, figure 7(*b*)), the existence of the streamwise vortices in the form of six petal 'mushrooms' in the lobed jet mixing flow can be seen clearly. The spanwise Kelvin–Helmholtz vortices rolling up at the lobe trough were found to be present as six crescents in these cross sections. With increasing streamwise distance, the 'mushrooms' grew up, which may indicate the process of formation and intensification of the streamwise vortices generated by lobed nozzles suggested by Werle *et al* (1987) and Eckerle *et al* (1990).

As the streamwise distance of the vortices increased to $X/D = 0.75$ ($X/H = 2.0$, figure 7(*c*)), the streamwise vortices generated by the lobed nozzle in the form of 'mushroom' structures kept on intensifying. Six new counter-rotating streamwise vortex pairs can also be found in

the flow field at six lobe troughs. Although the existence of horseshoe structures in the lobe trough had been conjectured by Paterson (1982) about 20 years ago, this is the best known visualization and provides unquestionable evidence of their existence.

At the location $X/D = 1.0$ ($X/H = 2.7$, figure 7(*d*)), some small-scale turbulent and vortical structures began to appear in the flow due to the mixing of the core jet flow with ambient flows. This verified the LIF visualization results for the axial slices which are shown in figures 4(*a*), 5(*a*) and 6(*a*). The interaction between the streamwise vortices and Kelvin–Helmholtz vortices made adjacent 'mushrooms' merge with each other, which indicated the process whereby the streamwise vortices deform the Kelvin–Helmholtz vortical tubes into pinch-off structures suggested by McCormick and Bennett (1994).

At the location $X/D = 1.5$ ($X/H = 4.0$, figure 7(*e*)) and $X/D = 2.0$ ($X/H = 5.7$, figure 7(*f*)), the 'mushroom' shaped structures in the flow field almost disappeared due to the mixing between the core jet flow and ambient flows. The
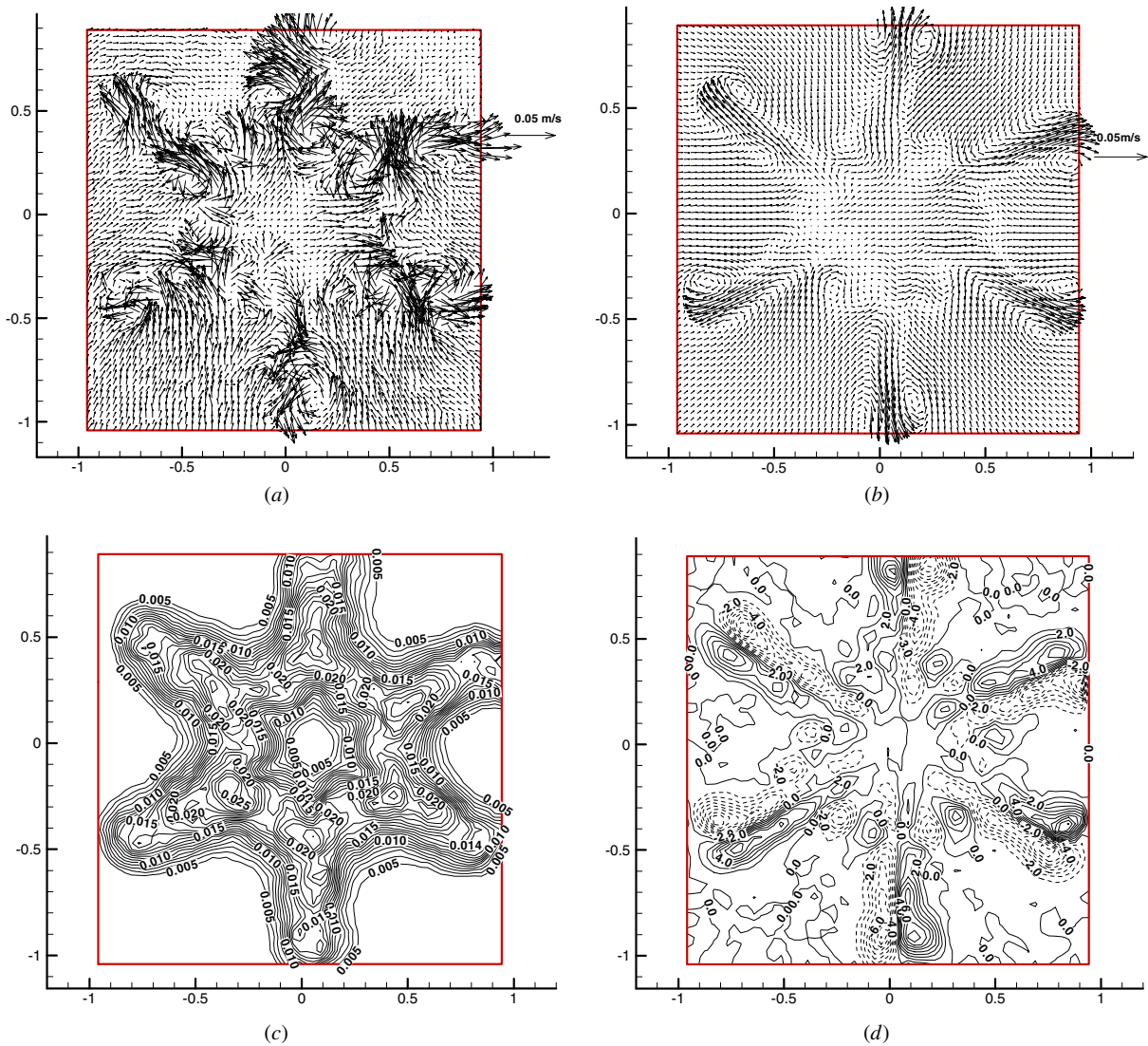
Figure 10. PIV measurement results for the lobed jet mixing flow for $(Re = 3000) X = 40$ mm: (*a*) the instantaneous velocity field, (*b*) the mean velocity field, (*c*) the turbulence intensity distribution and (*d*) the mean streamwise vorticity distribution.

flow field was almost fully filled with small-scale turbulent and vortical structures.

However, for the circular jet flow at the same Reynolds number, the jet flow is still in its laminar region at the location $X/D = 1.0$ (figure 8(*a*)). The spanwise Kelvin–Helmholtz vortices were found to begin to roll up at the location $X/D = 2.0$ (figure 8(*b*)). Neither small-scale turbulent structures nor small-scale vortical structures can be found in these cross planes for the circular jet flow.

Figures 9–12 shows the PIV measurement results for four typical cross planes of the lobed jet mixing flow, which include instantaneous velocity fields, mean velocity fields, turbulent intensity distributions and mean streamwise vorticity distributions. The large-scale streamwise vortices generated by the special geometry of the lobe nozzle can be seen clearly at the cross plane of $X/D = 0.5$ ($X/H = 1.3$, figure 9). The regions of intensive mixing (the high turbulence-intensity regions in figure 9(*c*)) were found to be in the same configuration as the trailing edge geometry of the lobed nozzle. Since the large-scale streamwise

vortices generated by the lobed nozzle are steady vortices, the streamwise vortices can be identified clearly in the mean velocity field and mean streamwise vorticity distribution.

When the streamwise distance had increased to $X/D = 1.0$ ($X/H = 2.7$, figure 10), the instantaneous velocity field was found to be more turbulent than that in the $X/D = 0.5$ ($X/H = 1.3$) cross plane (figure 9). However, the geometry of the lobed nozzle can still be identified from the velocity field. Just like in the LIF visualization results (figures 7(*c*) and (*d*)), the smaller scale streamwise horseshoe vortical structures can also be seen from the mean velocity field and mean streamwise vorticity field besides the six large-scale pairs of vortices generated by the lobed nozzle. The regions of intensive mixing were found to expand outwards and inwards from the turbulence intensity distribution (figure 10(*c*)).

When the streamwise distance downstream had increased to $X/D = 1.5$ ($X/H = 4.0$, figure 11) and $X/D = 2.0$ ($X/H = 5.3$, figure 12), the instantaneous velocity fields became much more turbulent, which indicates
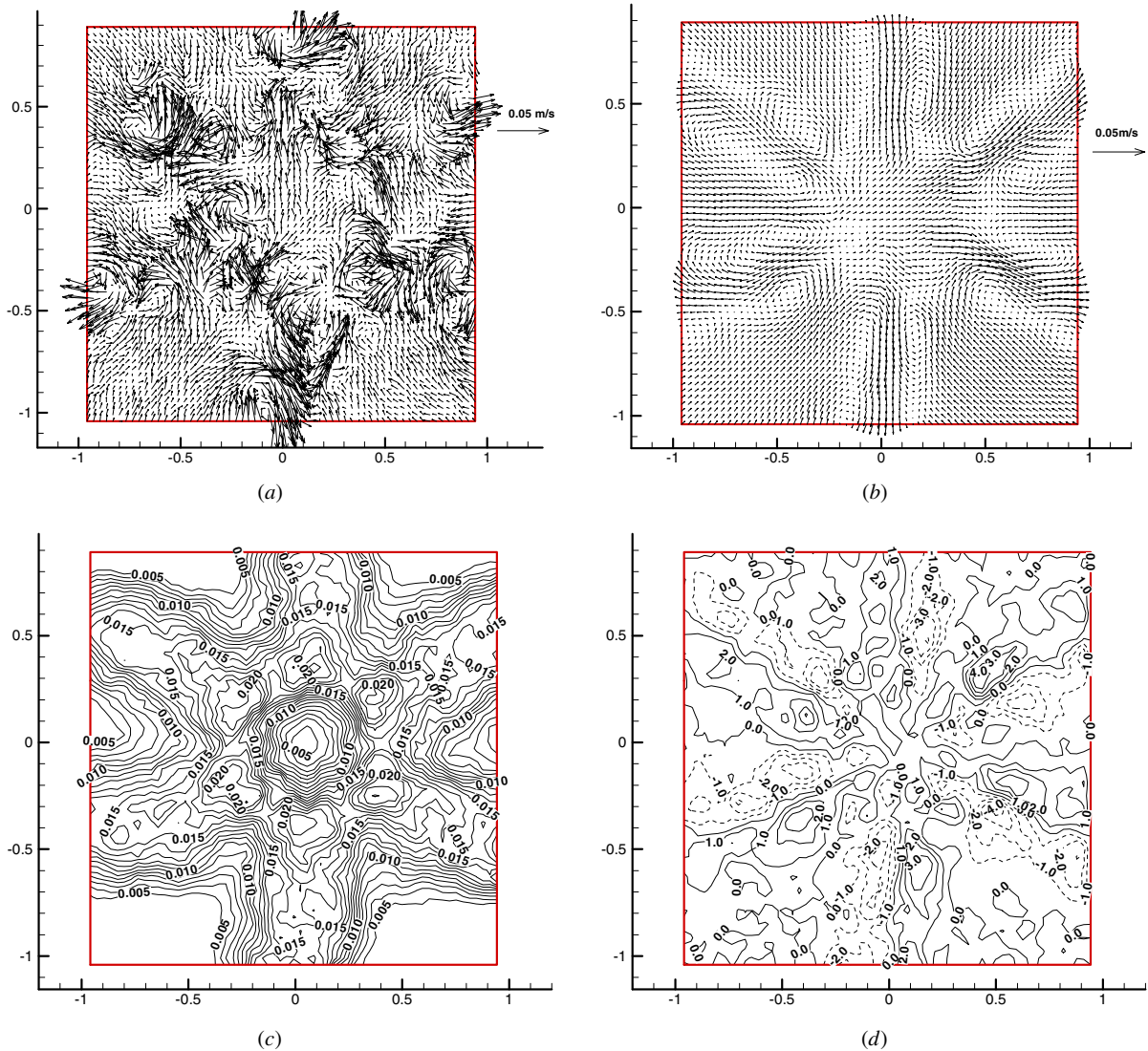
Figure 11. PIV measurement results for the lobed jet flow for $X = 60$ mm: (*a*) the instantaneous velocity field, (*b*) the mean velocity field, (*c*) the turbulence intensity distribution and (*d*) the mean streamwise vorticity distribution.

that more intensive mixing is occurring in these sections. The geometrical configuration of the lobed nozzle almost cannot be identified from the instantaneous velocity fields. The large-scale streamwise vortices generated by the lobed nozzle were found to break into many smaller vortices and the vorticity of the streamwise vortices was also found to have decayed a lot due to the mixing of the core jet flow with ambient flows. The regions of intensive mixing expanded much more seriously at these locations, which almost entirely filled the window studied.

3.3. The comparisons of mean velocity and turbulent intensity profiles in the lobed jet and circular jet flows

Figure 13 shows the mean velocity and turbulent intensity profiles of the lobed jet and circular jet flows at four locations downstream. At $X/D = 0.5$ ($X/H = 1.3$) downstream (figure 13(*a*)), the mean velocity profile of the lobed jet mixing flow in the lobe trough slice looks like a circular jet with smaller diameter. Two sharp peaks can be found

in the turbulent intensity profile, which correspond to the early rolling up of the spanwise vortices due to the Kevin–Helmholtz instability. The mean velocity of the lobed jet flow in the lobe peak slice was found to have a two-step distribution. The shear layer between the core jet flow and ambient flow seems to be divided into two sub-layers. The first sub-layer exists between the ambient flow and jet outer flow and the second sub-layer is between the jet outer flow and jet centre core flow. The doubled shear layers in the lobe peak slice result in four peaks in the turbulent intensity profiles. As was shown in the above LIF visualization results, the regions of intensive mixing (regions with normalized turbulent intensity values greater than 0.10) in the lobe peak slice are much wider than are those in the lobed trough slice. Since the circular jet is still in its laminar region, the amplitude of the peaks in the turbulent intensity profile for the circular jet flow is very small compared with that of those in the lobed jet mixing flow.

At the location $X/D = 1.0$ downstream ($X/H = 2.7$, figure 13(*b*)), the doubled shear layer of the lobed jet flow
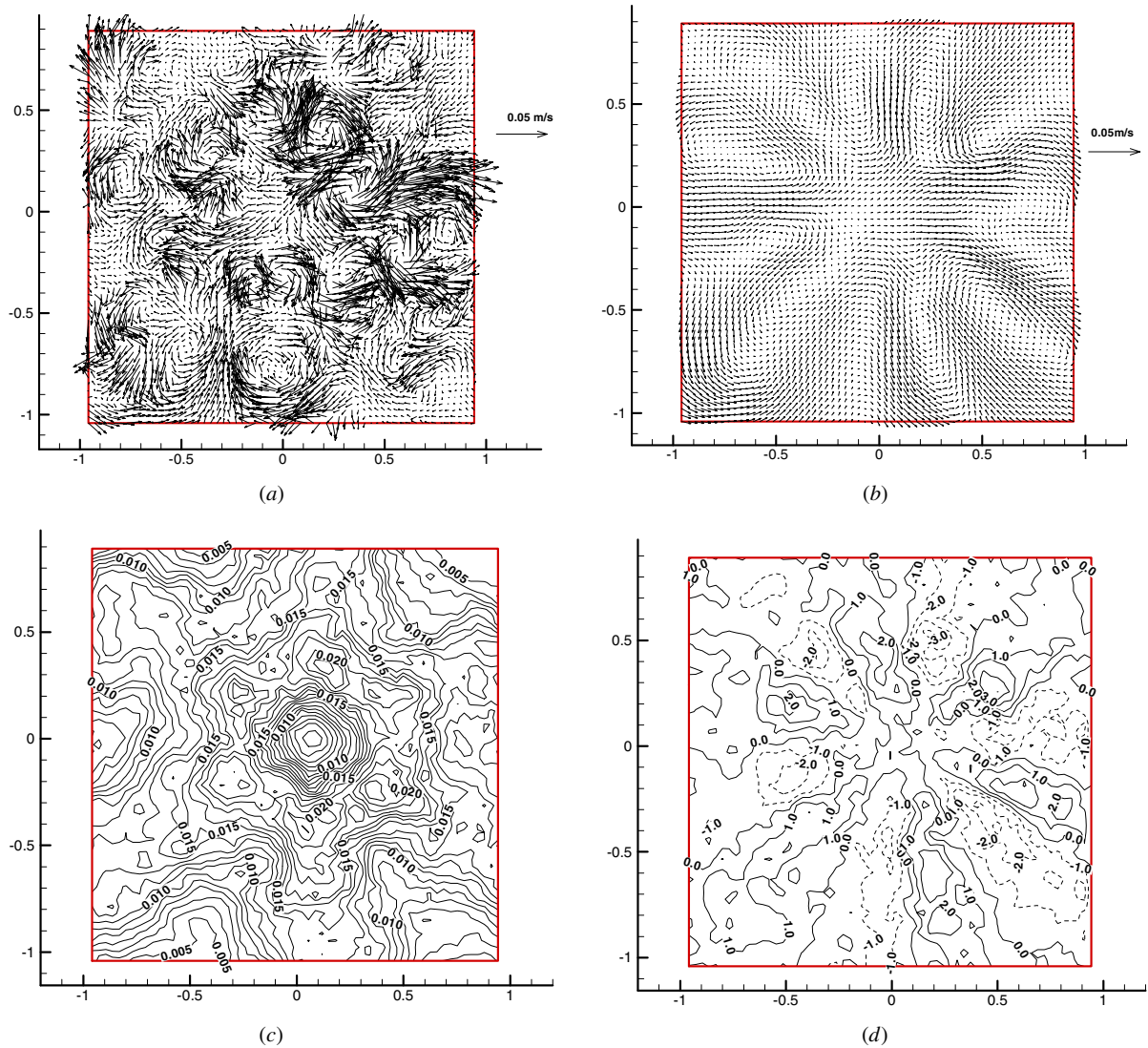
Figure 12. PIV measurement results the lobed jet mixing flow for $X = 80$ mm: (*a*) the instantaneous velocity field, (*b*) the mean velocity field, (*c*) the turbulence intensity distribution and (*d*) the mean streamwise vorticity distribution.

in the lobed peak slice had changed very seriously. The velocity ratio of the first sub-shear layer decreased, while that of the second sub-shear layer increased. This results in the turbulent intensity peaks in the first sub-layer decreasing and those in the second sub-layer increasing. The turbulent intensity peaks of the lobed jet flow in the lobe trough slice decreased with the growth in thickness of the shear layer. The magnitudes of the turbulent intensity peaks in the lobed peak slice and lobe trough slice are the same at this location. The circular jet is still in its laminar region at this downstream location, so the mean velocity and turbulent intensity profiles are almost the same as those at $X/D = 0.5$ ($X/H = 1.33$).

At the location $X/D = 2.0$ downstream ($X/H = 5.3$), the first sub-layer in the mean velocity profile of the lobe peak slice had dissipated so seriously that it almost cannot be identified. The patterns of the mean velocity and turbulent intensity profiles of the lobe jet flow in the lobe peak slice and lobe trough slice are very similar. Owing to the rolling up of the spanwise vortices caused by the Kelvin–Helmholtz

instability, the turbulent intensity peaks of the circular jet increased to the same level as those in the lobed jet mixing flow.

At the location $X/D = 3.0$ ($X/H = 8.0$), both the mean velocity and the turbulent intensity profiles of the lobed jet flow in the lobe peak slice and lobe trough slice were found to coincide with each other well. This may indicate that the effect of the special geometry of the lobed nozzle on the jet flow mixing had almost disappeared by this location. It also means that the enhancement of mixing caused by the special geometry of the lobe is almost finished by this location. The mixing between the core jet flow and ambient flow in the lobed jet flow farther downstream will occur by the same gradient-type mechanism as that for a conventional circular jet flow. McCormick and Bennett (1994) and Glauser *et al* (1996) had also got similar results in a planar lobed mixing flow and suggested that the region of maximum effectiveness for a lobed mixer is the first six lobe heights.

At this location, the amplitude of the turbulent intensity peaks of the conventional circular jet was found to be bigger
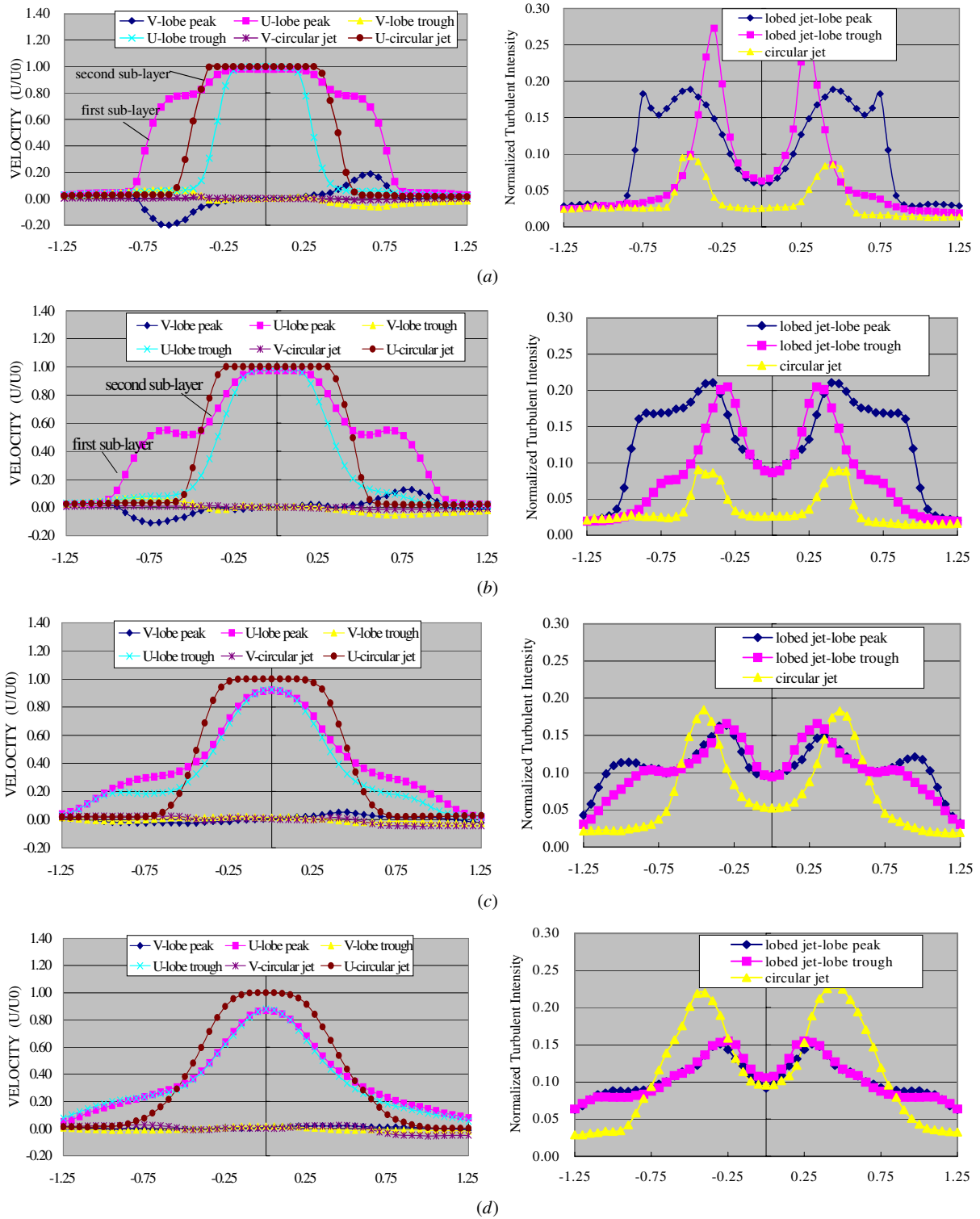
709

Figure 13. The mean velocity and normalized turbulent intensity profiles at four locations in the lobed jet mixing flow and circular jet flow ($Re = 6000$). (*a*) $X/D = 0.5$ ($X/H = 1.3$), (*b*) $X/D = 1.0$ ($X/H = 2.7$), (*c*) $X/D = 2.0$ ($X/H = 5.3$) and (*d*) $X/D = 3.0$ ($X/H = 8.0$),

than that of those in the lobed jet mixing flow. The lower turbulence intensity of peaks in the lobed mixing flow farther downstream is considered to be the result of the weaker (lower velocity ratio) doubled shear layers in the mean velocity profiles. McCormick and Bennett (1994) had also reported similar results in the farther field of a planar lobed mixer flow field.

3.4. The central line velocity decay

In order to give a more quantitative comparison of the mixing characteristics in the lobed jet mixing flow with those of conventional circular jet flow, the central line velocity decay in the conventional circular jet and lobed jet mixing flows are given in figure 14. From figure 14 it can be seen that the
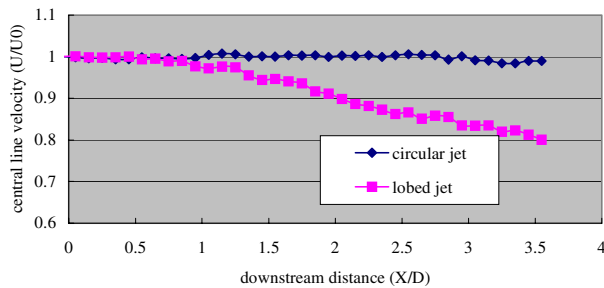
Figure 14. The central line velocity decay of the circular jet flow and lobed jet mixing flow ($Re = 6000$).

central line velocity of the circular jet flow remains almost constant in the region studied. Previous research had shown that the length of the potential core region in the conventional circular jet flow is also about 4.0–6.0 times the circular nozzle exit diameter. However, for the lobed jet flow, the central line velocity was found to begin to decay downstream of $X/D = 1.0$. This means that the length of the potential core region in the lobed jet flow is just about a quarter to a sixth of the conventional circular jet flow, which also indicated the better mixing performance of the lobed nozzle in the near field quantitatively

4. Conclusion

Both the planar LIF and PIV techniques were used in the present study to investigate the changes in the turbulent and vortical structures in the near field ($X/D < 3.0$) of a jet mixing flow caused by a lobed nozzle. The LIF visualization and PIV measurement results revealed the great differences in the turbulent structures and vortex scales between the lobed jet mixing flow and conventional circular jet flow. Compared with the circular jet flow, the lobed jet mixing flow was found to have a shorter laminar region, a smaller scale of the spanwise Kelvin–Helmholtz vortices, earlier appearance of small-scale turbulent and vortical structures and larger regions of intensive mixing in the near field of the jet flow. Besides the large-scale streamwise vortices generated by the special geometry of the lobed nozzle, the counter-rotating horseshoe vortices were also visualized clearly in the cross planes. It was also found that the length of the potential core region in the lobed jet mixing flow is only about a quarter to a sixth of that in the conventional circular jet flow. All these indicated that the a lobed nozzle gave better mixing than did a circular nozzle in the near field of the jet flow. The analysis to reveal the mechanism of the enhancement of the mixing performance of lobed nozzles and to optimize the design of lobed nozzles will be conducted in the future.

References

Belovich V M and Samimy M 1997 Mixing process in a coaxial geometry with a central lobed mixing nozzle *AIAA J.* **35** 838–41

Brink B K and Foss J F 1993 Enhancement mixing via geometric manipulation of a splitter plate *AIAA* 93-3244

Eckerle W A, Sheibani H and Awad J 1990 Experimental measurement of vortex development downstream of a lobed forced mixer *ASME* 90-GT-27

Elliott J K, Manning T A, Qiu Y J, Greitzer C S, Tan C S and Tillman T G 1992 Computational and experimental studies of flow in multi-lobed forced mixers *AIAA* 92-3568

Glauser M, Ukeiley L and Wick D 1996 Investigation of turbulent flows via pseudo flow visualization, part 2: the lobed mixer flow field *Exp. Thermal Fluid Sci.* **13** 167–77

Hu H, Kobayashi T, Wu S S and Shen G X 1999 Research on the vortical and turbulent structure changes of jet mixing flow by mechanical tabs *Proc. IME* **213** C, 321–9

Hu H, Liu H X and Wu S S 1996 Experimental investigation on the aerodynamic performance of the 2-D exhaust ejector system *ASME* 96-GT-243

Hu H, Saga T, Kobayashi T and Taniguchi N 1998 Evaluation the cross correlation method by using PIV standard image *J. Visualization* **1** 87–94

Hussain F and Husain H S 1989 Elliptic jets. Part 1: characteristics of unexcited and excited jets *J. Fluid Mech.* **208** 257–320

Liepmann D and Gharib M 1992 The role of streamwise vorticity in the near field entrainment of round jets *J. Fluid Mech.* **245** 643–68

McCormick D C and Bennett J C Jr 1994 Vortical and turbulent structure of a lobed mixer free shear layer *AIAA J.* **32** 1852–9

Paterson R W 1982 Turbofan forced mixer nozzle internal flowfield *NASA* CR-3492

Power G D, McClure M D and Vinh D 1994 Advanced IR suppresser design using a combined CFD/test approach *AIAA* 94-3215

Presz W M Jr, Renyolds G and McCormick D 1994 Thrust augmentation using mixer–ejector–diffuser systems *AIAA* 94-0020

Smith L L, Majamak A J, Lam I T, Delabroy O, Karagozian A R, Marble F E and Smith O I 1997 Mixing enhancement in a lobed injector *Phys. Fluids* **9** 667–78

Tillman T G and Presz W M Jr 1993 Thrust characteristics of a supersonic mixer ejector *AIAA* 93-4345

Ukeiley L, Glauser M and Wick D 1993 Downstream evolution of POD eigenfunctions in a lobed mixer *AIAA J.* **31** 1392–7

Ukeiley L, Varghese M, Glauser M and Valentine D 1992 Multifractal analysis of a lobed mixer flowfield utilizing the proper orthogonal decomposition *AIAA J.* **30** 1260–7

Werle M J, Paterson R W and Presz W M Jr 1987 Flow structure in a periodic axial vortex array *AIAA* 87-0160

Westerweel J 1994 Efficient detection of spurious vectors in particle image velocimetry data *Exp. Fluids* **16** 236–47

Willert C E and Gharib M 1991 Digital particle image velocimetry *Exp. Fluids* **10** 181–93